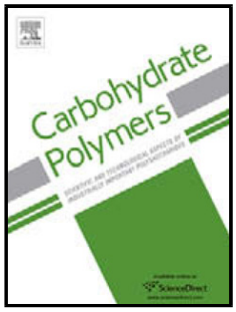

Title: Starch film-coated microparticles for oral colon-specific drug delivery

Authors: Jin Chen, Xiaoxi Li, Ling Chen, Fengwei Xie

PII: S0144-8617(18)30281-9
DOI: https://doi.org/10.1016/j.carbpol.2018.03.025
Reference: CARP 13375

To appear in:

Received date: 8-12-2017
Revised date: 10-3-2018
Accepted date: 13-3-2018

Please cite this article as: Chen, Jin., Li, Xiaoxi., Chen, Ling., & Xie, Fengwei., Starch film-coated microparticles for oral colon-specific drug delivery.*Carbohydrate Polymers* https://doi.org/10.1016/j.carbpol.2018.03.025

Starch film-coated microparticles for oral colon-specific drug delivery

Jin Chen [a,b], Xiaoxi Li [a], Ling Chen [a,*] and Fengwei Xie [b,#]

[a] *Ministry of Education Engineering Research Center of Starch & Protein Processing, Guangdong Province Key Laboratory for Green Processing of Natural Products and Product Safety, School of Food Science and Engineering, South China University of Technology, Guangzhou 510640, China*

[b] *School of Chemical Engineering, The University of Queensland, Brisbane, Qld 4072, Australia*

[*]Corresponding author. Tel.: +86 20 8711 3252; fax: +86 20 8711 3252. *Email address:* felchen@scut.edu.cn (L. Chen)

[#]Corresponding author. *Email addresses:* f.xie@uq.edu.au, fwhsieh@gmail.com (F. Xie)

Highlights:

- ✓ Film-coated microparticles were developed for colon-specific drug delivery
- ✓ Starch-coated films showed improved acidic and enzymatic resistance in the GI tract
- ✓ Native and retrograded starches were used as binders to reinforce the resistance
- ✓ Suitable molecular mass and high crystallinity of starch are important factors

ABSTRACT:

The aim of this study was to prepare and characterize a novel type of starch-coated microparticles (MPs) allowing site-specific delivery of bioactives to the colon. An oral colon-specific controlled-release system was developed in the form of MPs coated with a resistant starch (RS2/RS3) film (RS@MPs) through an aqueous suspension coating process. The RS2 was chosen from a high-amylose cornstarch with 88.5% digestion resistibility. The RS3 was prepared by a high-temperature/pressure (HTP) treatment, with the following of enzymatic debranching, and retrogradation, resulting in a dramatic increase in enzymatic resistance (RS3 content: 76.6%). RS@MPs showed 40.7% of 5-aminosalicylic acid release within 8h. The *in vivo* study of fluorescein-loaded RS@MPs indicated the high acidic and enzymatic resistibility of RS@MPs and a restrained release in the upper GIT. Therefore, RS@MPs has revealed to be a high potential system for accurately targeting bioactive compound delivery to the colon.

Keywords:

Resistant starch; aqueous suspension film coating; controlled release; oral colon-specific delivery.

Chemical compounds studied in this article

Starch (PubChem CID: 24836924); Water (PubChem CID: 962); Ethanol (PubChem CID: 702); Sodium hydroxide (PubChem CID: 14798); Acetic acid (PubChem CID: 176); Iodine (PubChem CID: 807); Potassium iodine (PubChem CID: 4875); D-Glucose (PubChem CID: 5793); Hydrochloric acid (PubChem CID: 313); Phenol (PubChem CID: 996); Sulfuric acid (PubChem CID: 1118); Potassium dihydrogen phosphate (PubChem CID: 516951); Dipotassium hydrogen phosphate

(PubChem CID: 24450); Citric acid (PubChem CID: 311); Dimethyl sulfoxide (DMSO) (PubChem CID: 679); Lithium bromide (PubChem CID: 82050); 5-aminosalicylic acid (5-ASA) (PubChem CID: 4075); Triethyl citrate (PubChem CID: 6506); Fluorescein isothiocyanate (FITC) (PubChem CID: 18730); Isoflurane (PubChem CID: 3763); Potassium chloride (PubChem CID: 4873); Sodium chloride (PubChem CID: 5234); 4',6-diamidino-2-phenylindole (DAPI) (PubChem CID: 2954).

Nomenclature

5-ASA	5-aminosalicylic acid
DAPI	4’,6-diamidino-2-phenylindole
DDSs	drug delivery systems
DMSO	dimethyl sulfoxide
FITC	fluorescein isothiocyanate
G50	Gelose 50
G80	Gelose 80
GIT	gastrointestinal tract
GPC	gel permeation chromatography
HACS	high-amylose cornstarch
HPMC	hydroxypropyl methylcellulose
HTP	high-temperature/pressure
IVIS	*in vivo* imaging system
MALS	multi-angle light scattering
M_n	number-average molecular weight
MPs	microparticles
M_w	weight-average molecular weight
NCS	normal cornstarch
OCT	optimum cutting temperature
PBS	phosphate buffered saline
PVP	povidone

RC	relative crystallinity
RDS	rapidly digestible starch
RS	resistant starch
RS@MPs	RS2/RS3 film-coated MPs
SCFA	short-chain fatty acids
SDS	slowly-digestible starch
SEM	scanning electron microscope
SGF	simulated gastric fluid
SIF	simulated intestinal fluid
WCS	waxy cornstarch
XRD	X-ray diffraction

1. Introduction

Emphasis has been placed on controlling the rate and/or site of bioactive compounds released from oral formulations for improving the therapeutic potentials (Sastry, Nyshadham & Fix, 2000). The colon is one area that would benefit from the development and use of such controlled release technologies. Colon-specific drug delivery systems (DDSs) have attracted many researchers due to distinct advantages such as near neutral pH, long transit time and reduced enzymatic activity (Haupt & Rubinstein, 2002). Delivery of active compounds to the colon can highly benefit for various applications, including the reduced administered dosage and side effect of anti-inflammatory drugs for local treatments, and the avoidance of unwanted digestion and the improved bioavailability of protein drugs for systemic absorption (Vinaykumar, Sivakumar, Tamizhmani, Rajan & Chandran, 2011).

An ideal colon-specific DDS should effectively suppress the release of active compounds in the stomach and small intestine. However, there could be some technical challenges, which are associated with the pH variations along the gastrointestinal tract (GIT), the digestion enzymes, and the long transit time (Hamman, Enslin & Kotzé, 2005). To overcome these obstacles, recent developments in polymeric materials offer opportunities to facilitate the advance of colon delivery carriers, including the use of bacteria-degradable, pH-sensitive, pressure-sensitive, and time-dependent coating polymers (Lin, Chen & Luo, 2007; Maroni, Zema, Del Curto, Foppoli & Gazzaniga, 2012; Said, 2005). Among materials susceptible to colonic biodegradation, the interest in polysaccharides has grown strongly in recent years because of their nontoxicity, safety, and good biocompatibility (Sinha & Kumria, 2001). In particular, starch, as the second abundant polysaccharide, has received considerable attention due to its low cost, diversity of source, and high

availability (Remon, Voorspoels, Radeloff & Beck, 1996). The starch that is not hydrolyzed in the small intestine but can be degraded by colon microorganisms, is considered as resistant starch (RS) (Thompson, 2000), which plays an important role in digestive physiology (Fuentes-Zaragoza, Riquelme-Navarrete, Sánchez-Zapata & Pérez-Álvarez, 2010). RS is normally classified into five main types, namely RS1, RS2, RS3, RS4, and RS5 (Fuentes- Zaragoza et al., 2011). These RSs can offer additional advantages of starch as colon-specific carrier materials, as the fermentation of RSs by anaerobic microflora in the colon can produce short-chain fatty acids (SCFA) (Rubinstein, 1990). These SCFA may play an important role in maintaining health by reducing the risk of diseases, such as inflammatory diseases, Type 2 diabetes, obesity, and heart disease (Ríos-Covián, Ruas-Madiedo, Margolles, Gueimonde, de los Reyes-Gavilán & Salazar, 2016).

For the purposes of controlled release and colon targeting, a well-accepted concept is to realize dosage forms to encapsulate active compounds with polymeric film coatings. Especially, much attention has been paid to the development of aqueous film coatings, instead of organic solvent, for safety, economic, and environmental reasons (Iyer, Hong, Das & Ghebre-Sellassie, 1990). Starch has been extensively evaluated for its film-forming ability as drug delivery coatings (Palviainen, Heinämäki, Myllärinen, Lahtinen, Yliruusi & Forssell, 2001). However, due to the hydrophilicity of starch and with the aim to avoid unwanted release of bioactives in the upper GIT, starches that are used as coating films need to be modified to possess particular features such as insolubility and impermeability (Cummings et al., 1996; Siccardi, Turner & Mrsny, 2005), resulting from the resistance to the acidic gastric pH or intestinal enzymes in the upper GIT (Chourasia & Jain, 2004). Up to now, most studies of starch-based films for colon-specific delivery have focused on blending commercially available polymers with starch derivatives to effectively control the physicochemical

properties of the blended coating films based on, *e.g.*, peas starch/ethylcellulose (Karrout et al., 2011), high-amylose starch/Surelease® (Freire, Podczeck, Veiga & Sousa, 2009), and amylose/Ethocel® (Milojevic et al., 1996). Yet, motivated by the low cost and nontoxicity of starch, few studies have concerned the preparation of starch-only coating films for effective colon-specific delivery based on, for example, chemically modified resistant starch acetate (RS4) (Chen, Li, Li & Guo, 2007; Chen, Li, Pang, Li, Zhang & Yu, 2007; Chen, Pu, Li & Yu, 2011; Li, Liu, Chen & Yu, 2011; Pu, Chen, Li, Xie, Yu & Li, 2011). Moreover, retrograded (recrystallized) starch (RS3) was also reported as a film coating material with a high potential for oral colon-specific delivery (Situ, Chen, Wang & Li, 2014). From this point, a colon-specific starch coating can be achieved merely by physically modified starch (retrograded RS3). Meanwhile, native starch granules can be a good source of RS2, which show high enzymatic resistance and can be hydrolyzed slowly by α-amylases (Chen, Liang, Li, Chen & Xie, 2016). The addition of particles to the coating may enhance its mechanical strength (Hari & Nair, 2016), which can help to counter intensive gastric digestion to avoid unwanted early release. Regarding this, if microparticles (MPs) loaded with bioactive compounds are coated with RS2/RS3 by an aqueous suspension film coating process, where the gelled starch molecules can aggregate with native starch particles that are suspended in the starch paste upon dehydration and drying, a colon-specific controlled-release system with high performance may be achieved. In this aqueous suspension system, native starch particles can maintain the high solid content while decreasing the viscosity of the suspension, thus reducing energy consumption (Borgquist, Zackrisson, Nilsson & Axelsson, 2002). In addition, due to the large size range of native RS2 particles, RS3 paste can also act as a binder to avoid the sediment of RS2 particles during the film coating process, and the reinforcement by RS2 granules has the high potential to allow the

formation of firm and compact films.

The present investigation attempts to develop a colon-specific controlled-release system in the form of RS2/RS3 film-coated MPs (RS@MPs) by an aqueous suspension film coating process. The approach consisted of two key parts. The first part is the preparation of RS2/RS3 film, which could be achieved simultaneously by the aqueous film coating technique using suspensions consisting of raw starch particles (RS2) and RS3 pastes. RS3 pastes can be prepared by a high-temperature/pressure (HTP) treatment, followed by enzymatic debranching, and retrogradation. An attempt was also made to estimate the resistance of RS2 and RS3 to the acidic gastric pH or intestinal enzymes in the upper GIT by studying their characteristics and the digestion resistibility. The second part is about release tests to verify the potential of colon-specific controlled release. 5-aminosalicylic acid (5-ASA) was chosen as an active compound to evaluate the release behavior of RS@MPs in *in vitro* experiments (*i.e.*, under the conditions of simulated human GIT). Besides, to understand the biocompatibility, the *in vivo* effectiveness of RS@MPs was also evaluated by an *in vivo* imaging system (IVIS) and tissue histospectroscopy in mice.

2. Materials and methods

2.1. Materials

Six commercially available cornstarches with different amylose/amylopectin ratios were used in this experimental work: (1) Gelose 80 (G80), supplied by Penford Australia Ltd. (Jannali, NSW, Australia); (2) Gelose 50 (G50), supplied by Penford Australia Ltd. (Jannali, NSW, Australia); (3) High-amylose cornstarch (HACS), supplied by Heilongjiang Huaneng Specialized Cornstarch Co., Ltd. (Heilongjiang, China); (4) Hylon V, supplied by National Starch and Chemical Co., Ltd.

(Bridgewater, NJ, USA); (5) Normal cornstarch (NCS), supplied by Inner Mongolia Yu Wang Biological Science Technology Co., Ltd. (Inner Mongolia, China); and (6) Waxy cornstarch (WCS), supplied by Qinhuangdao Lihua Starch Co., Ltd. (Hebei, China).

Potato amylose was purchased from the Heilongjiang Academy of Agricultural Sciences (Harbin, China); Pepsin and pancreatin from Sigma-Aldrich Co., LLC (Santa Clara, CA, USA); D-Glucose from Sigma Chemical Co. (St. Louis, MO, USA); Porcine pancreatic α-amylase and amyloglucosidase from Sigma-Aldrich (St. Louis, MO, USA); Glucose-oxidase peroxidase assay kit from Megazyme International Ireland Ltd. (Wicklow, Ireland); Pullulanase from Yulibao Biology and Technology Co., Ltd. (Guangzhou, China); 5-ASA from Yuancheng Technology Development Co., Ltd. (Wuhan, China); Microcrystalline cellulose from Anhui Shanhe Medicinal Accessary Material Co., Ltd. (Huainan, China); Medicinal starch from Defeng Starch Sugar Co., Ltd. (Shunde District, Foshan, China); Povidone (PVP) k 30 and hydroxypropyl methylcellulose (HPMC) from Guangzhou Feibo Botechnological Co., Ltd. (Guangzhou, China); Fluorescein isothiocyanate (FITC) from Biotium Inc. (Fremont, California, USA); Optimum cutting temperature (OCT) compound (McCormick Cryo-STAT) from Changzhou Philas Instrument Co., Ltd. (Jiangshu, China); and 4’,6-diamidino-2-phenylindole (DAPI) from Seajet Scientific Inc. (Beijing, China).

2.2. Characterization of native starches

2.2.1. Amylose content analysis

The amylose contents of native starches (G80, HACS, Hylon V, G50, NCS, and WCS) were determined using a modified method of ISO 6647-2:2007 of the International Standardization Organization (ISO, 2007). Specifically, 0.1 g (dry basis) of the starch was weighed and dissolved in 1

mL of ethanol and 9 mL of sodium hydroxide solution (1 mol/L), which was then heated in boiling water for 10 min. After cooling off, this solution was diluted to 100 mL in a volumetric flask with deionized water. An aliquot (2.50 mL) of this solution was then diluted with 25.00 mL of water, 0.50 mL of acetic acid solution (1 mol/L), 0.50 mL of I_2/KI solution (0.0025 mol/L I_2, and 0.0065 mol/L KI). The absorbance of this solution was read at 620 nm using an Evolution UV/vis spectrophotometer (Thermo Scientific, Waltham, USA). The amylose from potato (amylose content: 97.0%) was used for the calibration curve (R^2 = 0.9962).

2.2.2. Digestion resistibility in the upper GIT

The *in vitro* digestibility of six native starches (G80, HACS, Hylon V, G50, NCS, and WCS) was determined following the reported method (Thompson, Button & Jenkins, 1987) with modification. Duplicate 1 g (dry basis) of six native starches were weighed, suspended in 20 mL of simulated gastric fluid (SGF, pH 1.2) (Pu, Chen, Li, Xie, Yu & Li, 2011), and immediately placed in a dialysis bag (Spectra/Pro CE 131276T, molecular weight cutoff 8×10^3–10×10^3 g/mol), dialyzing against 500 mL of SGF in a beaker at 37 °C for 2 h. During this time, the loaded dialysis bag was shaken every 15 min to avoid starch sedimentation. After 2 h, a duplicate dialyzed starch sample was centrifuged, dried, ground and passed through a sieve (0.15 mm mesh size) for further use. These samples obtained from different starches were named as G80-SGF, HACS -SGF, Hylon V-SGF, G50-SGF, NCS-SGF, and WCS-SGF, respectively. While 1 mL of the dialysate samples were taken and analyzed for sugar release by the phenol-sulfuric acid method (Masuko, Minami, Iwasaki, Majima, Nishimura & Lee, 2005). Another duplicate sample was centrifuged, suspended in 20 mL of SIF. Then, the same procedure of the previous dialysis experiment was followed, except that SGF was

replaced by the simulated intestinal fluid (SIF, pancreatin, pH 6.8) (Pu, Chen, Li, Xie, Yu & Li, 2011) and the dialysis time was extended to 6 h. After that, these starch samples were mixed with ethanol to quench the enzyme activity, and then the dispersion was centrifuged at 3,000 g three times for 20 min. The sediments, named G80-SIF, HACS-SIF, Hylon V-SIF, G50-SIF, NCS-SIF, and WCS-SIF, respectively, were centrifuged, dried, ground for further use. The dialysate samples were also used for sugar release analysis. D-Glucose was used for the calibration curve in SGF (R^2 = 0.9991) and SIF (R^2 = 0.9995).

Granule morphology of six native starches and its hydrolyzed starch residues after 2 h of SGF and 6 h of SIF dialysis was studied using an EVO18 scanning electron microscope (SEM) (ZEISS, Germany) operated at a high voltage of 10.0 kV. Before SEM examination, the samples were coated with a gold thin film.

2.3. Preparation of RS3 samples

The modification involved the HTP treatment and the subsequent debranching of starch chains, according to our previously reported method (Situ, Chen, Wang & Li, 2014; Zhang, Chen, Zhao & Li, 2013). Considering the greater recrystallization tendency of amylose in gelled starch pastes (Whistler & BeMiller, 1997) and the requirement of the debranching treatment of amylopectin by pullulanase, Hylon V, with the amylose content of about 51%, was chosen.

50 g (dry basis) of Hylon V was dispersed in 200 mL water and cooked in a sealed reactor (Parr 4545, Parr Instrument Co., USA) at 110 °C under a pressure of 12.4 MPa with stirring at 200 rpm for 30 min. Then, the dispersion was cooled to 60 °C, and its pH value was adjusted to 5.0 using 10% (w/v) citric acid. Subsequently, different amounts of pullulanase (0, 50, 75, 100 and 200 ASPU/g dry

starch) were added for debranching the starch molecules at 60 °C under atmospheric pressure with stirring at 20 rpm for 2 h. The debranched starch was cooked at 100 °C for 10 min to stop the enzymatic hydrolysis, diluted to different concentrations of Hylon V paste (5%, 8%, 10%, 15%, and 20%, w/w), and then stored at 4 °C for 36 h (during which retrogradation occurred) for further use.

2.4. Characteristics of RS3 samples

2.4.1. In vitro digestibility of RS3 samples

The digestibility of RS3s was determined following a previously reported method (Chen, Liang, Li, Chen & Xie, 2016). Based on the rate of hydrolysis, starch was defined as rapidly-digestible starch (RDS, digested within 20 min), slowly-digestible starch (SDS, digested between 20 min and 120 min), and RS (undigested within 120 min).

2.4.2. X-ray diffraction (XRD)

XRD analysis was performed with an Xpert PRO diffractometer (PANalytical, Netherlands), according to the earlier method (Chen, Liang, Li, Chen & Xie, 2016). The relative crystallinity (*RC*) of each sample was calculated using a previous method of Hermans (Hermans & Weidinger, 1948). The ratio of the upper area (crystalline portion) to the total diffraction area (based on a linear baseline) was taken as the *RC* with the software MDI Jade 6.0.

2.4.3. Gel permeation chromatography (GPC) coupled with multi-angle light scattering (MALS)

A GPC system coupled with a MALS detector (632.8 nm, DAWN HELEOS, Wyatt Technology, Santa Barbara, CA, USA) and a refractive index (RI) detector (Optilab rex, Wyatt Technology) was

used to determine the weight-average molecular weight (M_w), number-average molecular weight (M_n), and molecular weight distribution. The GPC system consisted of a pump (1515, Waters, Milford, MA, USA), an auto-injector with a 0.1mL loop (717, Waters), and three columns (Sytyragel HMW7 GPC column, Sytyragel HMW6E GPC column, Sytyragel HMW2 GPC column, respectively, 7.8 × 300 mm, Waters). The data of light scattering was measured, collected and analyzed according to our earlier method (Situ, Chen, Wang & Li, 2014).

2.5. Preparation of the RS2/RS3 film-coated MPs (RS@MPs)

5-ASA-loaded MP cores (containing microcrystalline cellulose and medicinal starch in the ratio of 3:1 and the 5-ASA in the content of 16%, w/w) were obtained via extrusion–spheronization (Mini-250, Xinyite Co., Ltd., Shenzhen, China) (Pu, Chen, Li, Xie, Yu & Li, 2011). Different content of native starch particles (HACS, 3%, 5%, and 10%, w/w) were added to 5% (w/w) polymer pastes (RS3, PVP and HPMC), and 5% (w/w) triethyl citrate was added into the suspensions, which were then stirred for 8 h by a magnetic stirrer to form stable starch-based aqueous coating suspensions.

The 5-ASA-loaded MP cores were coated using a bottom-spray fluid-bed coater (Mini-XYT; Xinyite Technology Co., Shenzhen, China) to achieve the coated-film thickness of 16–50% (w/w, the dry weight gain of MPs) (Pu, Chen, Li, Xie, Yu & Li, 2011). The process parameters were as follows: motor speed at 1500–2000 rpm; inlet temperature at 55–60 °C; temperature of bioactive component-loaded MPs at 28–31 °C; spray rate of coating dispersion at 1–1.5 mL/min; atomization pressure at 0.15–0.2 MPa; and fluidization pressure at 0.04 MPa.

2.6. In vitro release testing

The release of 5-ASA from the different film-coated MPs (PVP, HPMC, and RS2/RS3) was carried out using a dissolution rate test apparatus (RCZ-8B, Tianda Tianfa Co., Ltd., Tianjin, China) (100 rpm, 37 °C) according to the USP23 dissolution method (Labastie, Solange, Brandão & Cumps, 1998). The MPs were incubated in SGF for the first 2 h, then in SIF for another 6 h. 5 mL of each sample was taken at appropriate time intervals and analyzed for 5-ASA content using a UV spectrophotometer (Unico, UV-3802, Shanghai, China). The calibration curves of 5-ASA for SGF (R^2 = 0.9999) and SIF (R^2 = 0.9990) were used for the determination of 5-ASA release percentage.

2.7. In vivo release testing in mice and the related morphological observation

The FITC-loaded RS@MPs (loaded content: 2%, w/w) were prepared by the method described in Section 2.5 with minor modifications to fit the GIT transition time in mice. According to our preliminary tests, the gastric residence time in mice was 2 min, and the small intestinal residence time in mice was 42 min. After 44 min, RS@MPs entered the colon physiological environment.

Three eight-week-old male nude mice (NO.11400700045743, Beijing Vital River Laboratory Animal Technology Co., Ltd., Beijing, China), each weighing 18–22 g, were fasted for 24 h before the test. FITC-loaded RS@MPs (80 mg/kg of rat) in 0.1 mol/L phosphate buffered saline (PBS) buffer (pH 7.4) were injected into one mouse by intragastric administration via polyethylene tubing (experiment group). The other two mice were injected with an equivalent amount of PBS solution (blank control group) and uncoated FITC-loaded MPs in PBS buffer (reference group), respectively. Then, the three treated mice were anesthetized with isoflurane immediately and subject to spatiotemporal detection of FITC transition along the GIT using an IVIS (IVIS 200, Xenogen Co.,

Ltd., Alameda, Canada). *In vivo* fluorescent images (the excitation spectrum: 445-490nm; the emission spectrum: 515-575nm) were captured at the predetermined time points (10 min, 20 min, 50 min, 80 min, 120 min, and 180 min) after the intragastric administration of FITC-loaded MPs to the experimental mice.

36 thirteen-week-old Institute of Cancer Research (ICR) mice (NO.11400700045743, Beijing Vital River Laboratory Animal Technology Co., Ltd., Beijing, China), half male and half female, each weighing 18–22 g, were fasted for 24 h before the test. The FITC-loaded RS@MPs (80 mg/kg of rat, the experiment group) and uncoated FITC-loaded MPs (80 mg/kg of rat, the reference group) were orally administered to the stomach via polyethylene tubing. At certain times after their oral administration (10 min, 20 min, 40 min, 80 min, 4 h, and 24 h), the rats were sacrificed by cervical dislocation, and the tissues of the stomach, small intestine, and colon were obtained. Then, the OCT compound (McCormick Cryo-STAT)-embedded tissue sections of the stomach, small intestine, and colon of the rats were sliced into 6 μm depth by a cryostat microtome (Shandon cryotoZFE, Thermo Fisher Scientific Co., Ltd., Waltham, USA) at −20 °C. Afterwards, the section slides were dyed with DAPI for histospectroscopy using a two-photon confocal laser scanning microscope (Zeiss 710 NLO, Zeiss, Germany). The process parameters were as follows: wavelength filter: 491–545 nm; objective lens: Plan-Apochromat 20x/0.8 M27; pinhole detector: 150 μm; pixel dwell: 1.58 μs; repeated scanning time: line 2.

2.8. Statistical analysis

The mean values and differences were analyzed using Duncan's multiple-range test. Analysis of variance (ANOVA), followed by the least significant difference test (LSD-test), was performed using

SPSS (Version 22.0) software. The significance level was set at $p < 0.05$.

3. Results and discussion

3.1. Characteristics and in vitro digestion analysis of native starches

Being administrated orally, DDSs face several physiological challenges such as the acidic pH in the stomach and the digestive enzymes in the intestine (Hamman, Enslin & Kotzé, 2005), which could require the resistance of drug carrier materials to protect the carried pharmacologically active agents. As seen from Table 1, regardless of amylose content, all native starches showed high enzyme-resistance (Undigested starches: 85.6–89.6%), suggesting they are good sources of RS2. Still, there was a significant difference in RS content among native starches with different amylose contents. Specifically, native starches with a high amylose content (≥ 50%) were less susceptible to acid or enzymes than others with high amounts of amylopectin (NCS and WCS). This difference can be explained by the higher amount of B-type crystalline structure with an increase in amylose content (Cheetham & Tao, 1998), which was intrinsically resistant to acid (Gérard, Colonna, Buléon & Planchot, 2002; Vermeylen, Goderis, Reynaers & Delcour, 2004) or enzymatic degradation (Jane, Wong & McPherson, 1997). Depending on the packing of the amylopectin side chains into double helices, the starch crystalline structure can be normally described as either A, B, or C (Luengwilai & Beckles, 2009). Compared with A-type crystalline structure in NCS and WCS (Cheetham & Tao, 1998), B-type crystallites have been proposed to be accompanied by a higher amount of long chains and more branch points in non-crystalline regions, leading to high-density amorphous regions and stable crystallites, which resist enzymatic hydrolysis (Jane, Wong & McPherson, 1997). Besides, the B type has been assumed to contain larger blocklets supposedly arrange in a peripheral ring of starch

granules, which acts as a barrier to hydrolytic enzymes (Oates, 1997). However, as H_3O^+ ions can diffuse easily within the granule, this organization could not account for the behavior of acid hydrolysis. The acid resistance of B-type crystallites may result from their intrinsic stability, three-dimensional size, their size along the *c*-axis, and/or a greater perfection (Planchot, Colonna & Buleon, 1997). Furthermore, especially after 6 h of incubation in SIF, their resistance decreased with a higher amylose content with the same crystalline type among native starches. Since the amount of double-helical order in native starches should be strongly correlated to the amylopectin content, the granule's crystallinity decreased with amylose content (Gernat, Radosta, Anger & Damaschun, 1993), thus, higher susceptibility to enzymatic degradation.

Table 1 Amylose content and *in vitro* digestion of native starches

Native starches	Amylose (%)	Digested starch in SGF (%)	Digested starch in SIF (%)	Undigested starch (%)
G80	80 ± 2^{a}	0.25 ± 0.02^{b}	11.5 ± 0.2^{c}	88.3 ± 0.2^{c}
HACS	72 ± 2^{b}	0.23 ± 0.01^{b}	11.3 ± 0.2^{cd}	88.5 ± 0.3^{cd}
Hylon V	51 ± 2^{c}	0.23 ± 0.02^{bc}	11.1 ± 0.1^{d}	88.7 ± 0.1^{d}
G50	50 ± 2^{c}	0.24 ± 0.01^{b}	10.1 ± 0.1^{e}	89.6 ± 0.1^{e}
NCS	28 ± 1^{d}	0.32 ± 0.01^{a}	14.1 ± 0.2^{a}	85.6 ± 0.2^{a}
WCS	1 ± 0.3^{e}	0.26 ± 0.01^{b}	12.5 ± 0.1^{b}	87.3 ± 0.1^{b}

Values are means of three determinations (±standard deviation); values followed by the different letters within a column differ significantly ($p < 0.05$).

The degree of hydrolysis can be influenced by both the granule parameters (size and surface features) and internal structure of starch. From SEM micrographs (Fig. 1), all native cornstarch

granules were irregular in shape and displayed a similar range of sizes (3-26 μm). In addition, the surfaces of high amylose starches (G80, HACS, Hylon V, and G50) were comparatively smooth without scratches, whereas small pores and pits were found randomly distributed on the surface of NCS and WCS granules. These surface pores were suggested to be openings to channels that penetrate in a roughly radial direction through the granule (Fannon, Shull & BeMiller, 1993).

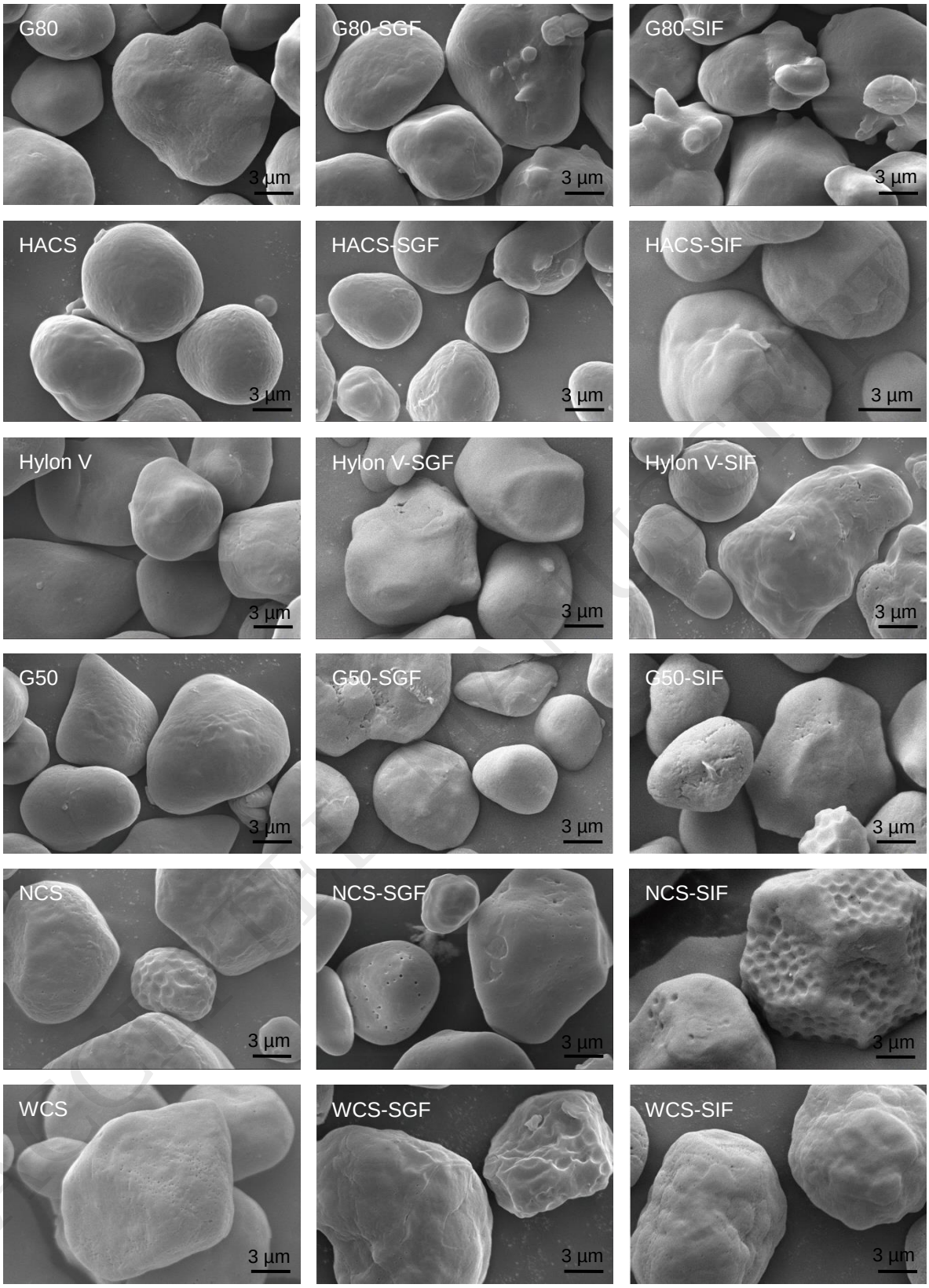

Fig. 1. SEM images of native and hydrolyzed starch residues.

The susceptibility of starch granules can be classified by the manner and degree by which the granules are eroded and corroded. As seen from SEM images, the surface erosion of all six hydrolyzed starch granules was marginal, which was in accordance with the high resistance of native starches (Table 1). Yet, the degree of hydrolysis varied among different starch granule features and was intensified by the subsequent enzymatic degradation after acidic hydrolysis. After 2 h in SGF and 6 h in SIF of incubation, no apparent hydrolysis of G80 and HACS was seen, with the surfaces becoming slightly rougher with some pitting (G80-SIF and HACS-SIF in Fig. 1) but still resembling those of the native starch granules. In contrast, more apparent hydrolysis of G50 and Hylon V was observed as more rugged granule surfaces with increased pinholes and furrows after incubation in SGF and SIF. This difference existed despite that G50 and Hylon V had a higher resistance than G80 and HACS. However, compared with high amylose starches (G80, HACS, Hylon V, and G50), the erosion profiles of NCS and WCS were much obvious from the increased surface roughness and the formation of hole depressions in many granules (NCS-SIF, WCS-SGF, and WCS-SIF in Fig. 1). For high-amylose starches, the intensity of digestion could be tempered due to the smooth surface without pores as the amylose molecules fill the gaps/spaces (Bertoft & Manelius, 1992), which was another reason for lower susceptibility to digestion. Thus, high-amylose starches (G80, HACS, Hylon V, and G50) with high acid/enzyme-resistance can be good choices as suspension particles in the film-coating process. Also, with the consideration of comparatively low price and low susceptibility to corrosion, HACS was finally chosen as suspension particles to increase the RS content of RS@MPs.

3.2. Preparation and characteristics of RS3 samples.

Owing to the necessary resistibility of starch-based films to realize the colon-specific delivery by the coated MPs, RS3s with different characteristics have been prepared by physical modification. Because of the significant roles of pullulanase activity and the starch concentration of paste in the formation of RS3s (Situ, Chen, Wang & Li, 2014; Zhang, Chen, Zhao & Li, 2013), these two parameters were exclusively investigated to compare the preparation and characteristics of RS3 samples. Fig. 2 A-B show the RDS, SDS, and RS results of modified starch samples. Compared with native Hylon V, an apparent increase in RS content and a decrease in RDS content were observed for all the modified samples. These results demonstrated that the digestion resistibility of starch could be improved by the HTP and debranching treatments and the following retrogradation and drying processes. Through the process of recrystallization, the gelatinized starch (amylose and debranched short starch molecules) can be transformed from an amorphous state to a more ordered or crystalline state, which has a high enzymatic resistance (Sajilata, Singhal & Kulkarni, 2006). However, no apparent increase in SDS content was seen for these samples, and in most cases, there was a lower SDS content than that of Hylon V (SDS: 9.8±0.6%). This trend of SDS variation was not surprising since amylopectin had a major impact on the inherent slow digestion property of starches (Zhang, Ao & Hamaker, 2006). After treatment, the branched structure of amylopectin was destroyed, so less SDS chains were recrystallized and formed.

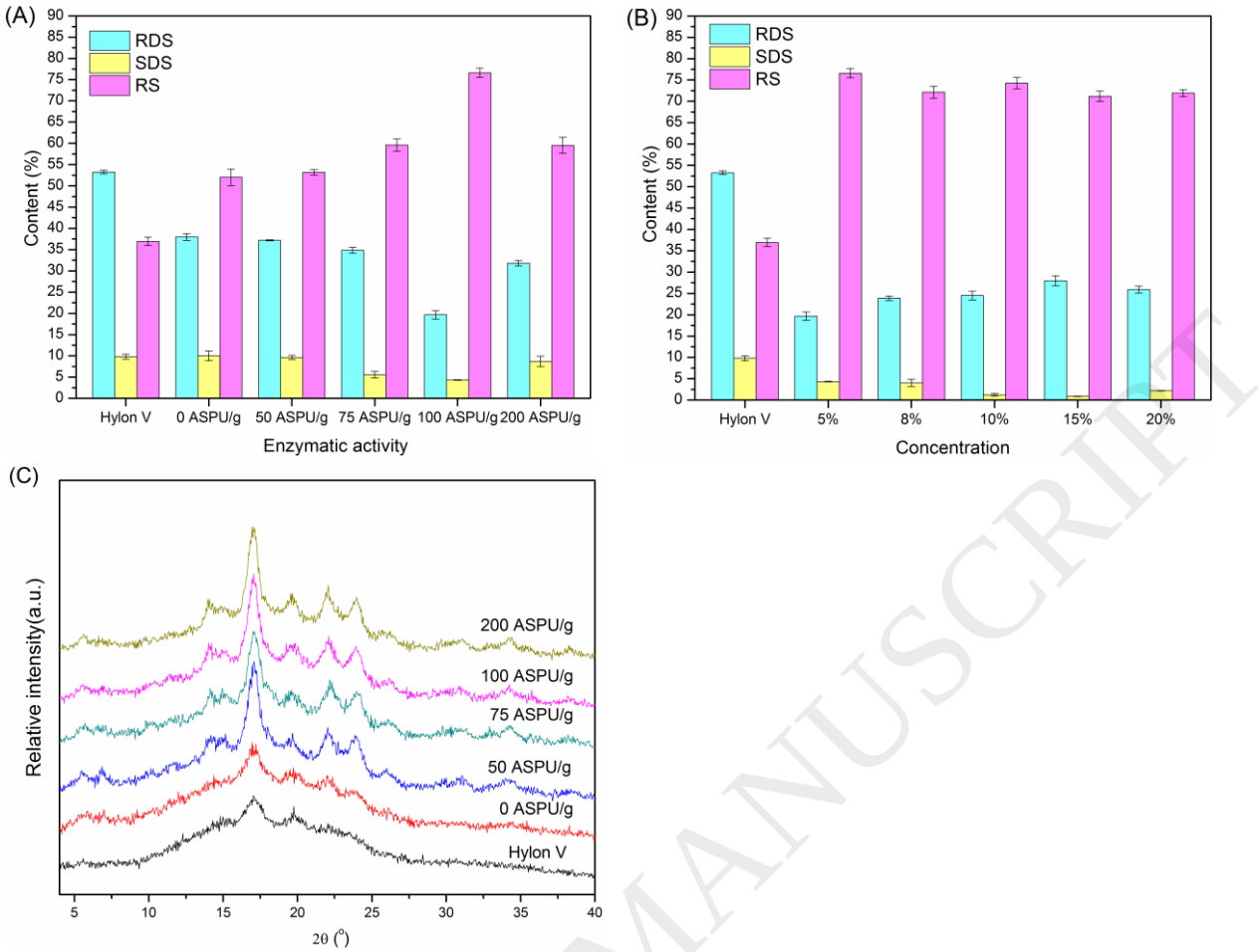

Fig. 2. Effect of enzymatic activity (A) and starch concentration of paste (B) on the RDS, SDS, and RS contents of the debranched HTP-treated Hylon V; and XRD of different RS3 samples (C). The standard deviations of (A) and (B) were within 1.9% and 1.4%, respectively.

Fig. 2A shows the effect of enzymatic activity on the formation of RDS, SDS, and RS when the starch concentration was fixed at 5% (w/w). As seen in Fig. 2A, debranching could further increase the RS content compared with the samples with only HTP treatment (0 ASPU/g). Regarding this, debranching would give starch chains a greater chance to align and aggregate to form ordered structures, thereby leading to a higher RS content. Increasing the pullulanase activity raised the RS content until a maximum of 76.6% (±1.1%) RS was reached at 100 ASPU/g. When the pullulanase

content was increased to 200 ASPU/g, the RS content was reduced to 59.5% (±1.9%). The HTP and debranching treatments with a suitable amount of pullulanase could lead to the gelatinization and destruction of starch granules, resulting in an irreversible swelling and degradation of starch molecules. Then, during retrogradation, some of the degraded starch chains of suitable molecular weight could reassociate to form tightly packed structures stabilized by hydrogen bonding, which would render α-1,4 glucosidic linkages inaccessible to enzymes to hydrolyze, leading to a higher RS3 content. However, with a further increase in pullulanase activity, the starch molecules could be degraded further, and these molecules could not preferably form tightly-packed ordered aggregations; thus, a decrease in RS content resulted (Pongjanta, Utaipattanaceep, Naivikul & Piyachomkwan, 2009).

On the other hand, for the samples subject to the HTP and branching treatments at 100 ASPU/g, a paste starch concentration of 5% could lead to the maximum RS content. The RS content just declined slightly with the increased starch concentration (Fig. 2B), which suggested that a high starch concentration might hinder the formation of RS. This result can be explained by the diffusion of starch molecules during retrogradation. When the starch concentration was low, despite the less chance of starch molecules to reassociate, there could be more free space for starch chains to entangle and orientate for more perfect crystalline structures, leading to high enzymatic resistibility (Ottenhof & Farhat, 2004). In contrast, a higher starch concentration resulted in an increased viscosity, which could hinder the movement and orientation of starch chains. In this way, imperfect crystallites tended to form, resulting in a lower RS content. Since a starch concentration of 5% was favorable for RS3 formation, this concentration of RS3 paste was selected for the further preparation of RS2/RS3 film-coating suspension.

The enzymatic resistibility of RS3 was related to the molecular structure (linear or branching, and molecular weight) of starch during retrogradation and the ordered structure of retrograded RS3. Here, RS3 samples with different degrees of pullulanase activity were characterized for molecular weight and crystalline structure. Fig. 2C shows the XRD patterns of native and RS3 samples. Their calculated *RC* values are shown in Table 2. It can be seen that all the samples (Hylon V and RS3s) displayed a B+V type hybrid polymorph, with main diffraction peaks of a typical B-type crystalline structure at around 5.6°, 17°, 22.0°, 23.4°, and 26.0° (Luengwilai & Beckles, 2009), and one peak at 19.8°, which was related to the V-type crystalline structure (Buléon, Colonna, Planchot & Ball, 1998). The V-type crystalline was caused by amylose–lipid complex, which has been proposed to hinder the enzymatic hydrolysis by covering the starch granule surface, leading to an increased content of RS (Crowe, Seligman & Copeland, 2000; Cui & Oates, 1999; Tufvesson, Skrabanja, Björck, Elmståhl & Eliasson, 2001). Compared with the XRD pattern of native Hylon V starch, most of the peaks (B+V) of RS3 samples became clearer. Their intensity was slightly enhanced after only HTP treatment and increased gradually as the degree of debranching increased. However, when the pullulanase activity reached 200 ASPU/g, the intensity of XRD pattern was slightly decreased. These results were further revealed and supported by *RC* data. The *RC* of native Hylon V was 10.30%, and increased after the HTP treatment and further increased by debranching. The maximum *RC* was 78.34% at 100 ASPU/g pullulanase activity. The result of the crystalline structure is consistent with the analysis of RS content (Fig. 2A).

Table 2. GPC-MALS results and crystallinity of debranched HTP-treated RS3 samples

Pullulanase activity (ASPU/g)	M_w (g/mol)	M_w/M_n	$< 10^5$ [B] (%)	10^5–10^6 (%)	10^6–10^7 (%)	$>10^7$ (%)	*RC* (%)
Hylon V	6.385×10^6 (1% [A])	4.085 (2%)	0	31.62	50.16	18.22	10.30
0	1.567×10^6 (1%)	2.991 (2%)	0	71.79	25.38	2.83	36.55
50	3.516×10^5 (0.7%)	2.030 (1%)	0	95.84	4.16	0	71.06
75	2.175×10^5 (0.7%)	1.987 (2%)	36.40	61.26	2.34	0	72.20
100	2.067×10^5 (1%)	1.534 (2%)	21.81	76.74	1.45	0	78.34
200	1.329×10^5 (1%)	1.369 (2%)	33.22	66.78	0	0	76.59

[A] Precision of global fit. [B] means the molecular distribution of M_w with units (g/mol).

Table 2 shows the GPC-MALS results of native Hylon V and modified starches. After the HTP treatment, the M_w of Hylon V was reduced sharply from 6.385×10^6 to 1.567×10^6 g/mol. The M_w of HTP-treated samples was further reduced distinctly with debranching, and this value was even lower with more intensive debranching. This result confirmed the degradation of starch molecules by HTP and debranching. With the branching process, the M_w/M_n value, which reflects the polydispersity of molecular weight, was also seen to be decreased, suggesting the increased uniformity of molecular weight of modified starches. Moreover, Table 2 shows that with increased debranching, the high molecular fractions ($M_w > 10^7$ g/mol and $10^6 < M_w < 10^7$ g/mol) gradually decreased to nil, while the low molecular fraction ($M_w < 10^5$ g/mol) was substantially increased. Combined with the RS content and M_w parameters, it can be concluded that the starch molecules with $M_w = 2.067\times10^5$ g/mol favored the alignment and arrangement of double helices to form ordered structures during retrogradation. Moreover, the large amounts of ordered crystalline structure (B+V type) could be the main reason for the enhanced starch resistance to enzymatic digestion.

3.3. RS2 as the suspended particles and RS3 paste as the binder for RS2/RS3 film-coated MPs (RS@MPs)

According to the results in Section 3.2, 5% concentration of RS3 paste with M_w = 2.067×10^5 g/mol was selected for the preparation of RS2/RS3 aqueous film-coating suspension. To study the potential of RS3 starch paste as a binder to prepare a compact and firm film, the release behavior of 5-ASA-loaded RS@MPs was compared with those MPs coated by films using two typical binder polymers (PVP and HPMC) incorporated with RS2 granules.

As seen in the Fig. 3A, the release behavior of RS@MPs was similar to those film-coated MPs with PVP or HPMC, suggesting that the binding capability of RS3 paste was comparable to that of typical polymer binders. However, all of three film-coated MPs (with RS2/RS3, RS2/PVP, or RS2/HPMC) showed a rapid release, especially in the case of RS3 paste as the binder. The release percentage of 5-ASA from RS@MPs was up to 68.6 % (±2.6%) at the end of 2 h in SGF, indicating the inability for colon-targeted delivery. To inhibit the rapid release of bioactive component, the film coating process was improved by a double-coating method, *i.e.*, 50% of suspension used for film firstly, and then the left 50% of suspension used for coating on top of the prior formed film. Compared with the single-coating method, the double-coating method of RS@MPs significantly reduced the release rate, with reduced release percentage in SGF (40.1±0.6%) and reduced total release percentage (54.5±1.0%) after another 6 h in SIF, showing a good potential of colon-specific delivery. Still, there was a burst release from 5-ASA loaded RS@MPs with the release percentage up to 35.0 % (±2%) at the end of 1 h in SGF. This fast release could be ascribed to the bioactive component molecules that were mostly loaded at or near the surface of the MPs (Woo, Jiang, Jo & DeLuca, 2001). In the following experiments, the double-coating method was used for a better

release behavior of RS@MPs.

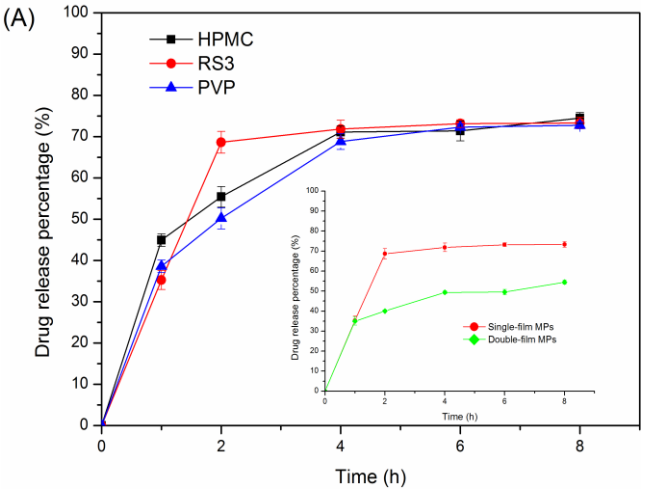

Concentration of polymers: 5% (w/w); concentration of HACS: 5% (w/w); 5-ASA load: 16% (w/w); thickness of film coating: 50% (w/w)

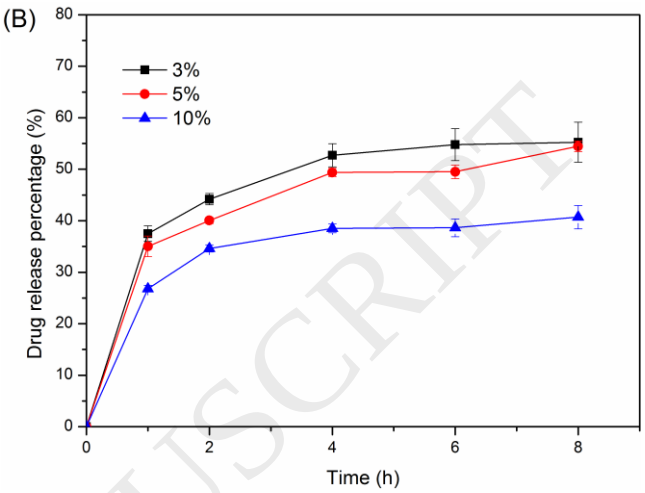

Concentration of Hylon V paste: 5% (w/w); 5-ASA load: 16% (w/w); thickness of film coating: 50% (w/w)

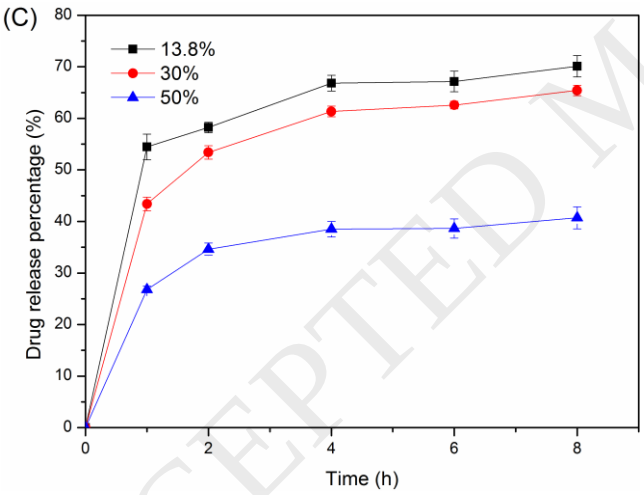

Concentration of Hylon V paste: 5% (w/w); concentration of HACS: 10% (w/w); 5-ASA load: 16% (w/w)

Fig. 3. Effects of polymers (PVP, HPMC, and RS3) (A), RS2 granule content (B) of RS2/RS3 coating film, and film coating thickness (C) on the release behavior. The standard deviations of (A), (B) and (C) were within 2.6%, 3.9% and 2.5%, respectively.

3.4. In vitro 5-ASA release from RS@MPs

To optimize the colon-specific release property of 5-ASA loaded RS@MP delivery system further, the effects of RS2 (HACS) granule content and film coating thickness on the 5-ASA release behavior from the RS@MPs in the simulated human GIT were investigated, with the results presented in Fig. 3. As another main film component, the content of RS2 granules may play a vital role in the film quality. Therefore, the *in vitro* release of 5-ASA from RS@MPs containing different content (3–10%, w/w) of HACS granules were evaluated, and the results are shown in Fig. 3B. It can be seen that the 5-ASA release in SGF and SIF decreased with the increased HACS granules content. This can be explained by the high acidic and enzymatic resistance of HACS granules (Table 1) and the enhanced mechanical strength of RS2/RS3 film by the addition of HACS granules (Hari & Nair, 2016). With the increased content of HACS granules, the RS2/RS3 film was much firmer and suffered less erosion in SGF and SIF. Thus, the diffusion of 5-ASA was hindered and less released from RS@MPs with a higher RS2 content. When the content of HACS granules was 10%, the release percentage from RS@MPs was 40.7% (±2.3%) for 8 h in the upper GIT, indicating that these RS@MPs could target the bioactive components to the colon. Therefore, a HACS granule content of 10% should be suitable for preparing RS@MPs with good colon-targeted controlled-release performance.

The coating film thickness could also be an important parameter to control the release behavior of RS@MPs. Fig. 3C shows the percentages of release from RS@MPs with different thicknesses of film coating (13.8%–50%) when the content of HACS granules was fixed at 10%. As expected, the release percentage decreased with increasing the film-coating thickness. This was because the increased film-coating thickness could significantly increase the length of the diffusion pathways for

the bioactive component. With the consideration of colon-targeted release performance, a film-coating thickness of 50% was preferable. The results discussed above (Fig. 3) have shown that the colon-targeted release behavior of RS@MPs could be well adjusted by the formulation of suspensions and process parameters.

3.5. In vivo release fluorescein from RS@MPs

We also assessed the *in vivo* behavior of RS@MPs in terms of the residence time of formulation in different parts of the GIT. By IVIS, the FITC release behavior from RS@MPs in mice was studied. Fig. 4 shows the *in vivo* images of FITC distribution at different times in nude rats after administration of PBS solution (left), FITC-loaded uncoated MPs (middle), and RS@MPs (right). It can be seen that there was no fluorescent spot found on the nude mice injected by PBS solution for the whole experiment period (from 10 to 180 min), indicating no autofluorescence phenomenon occurred in nude mice under IVIS. As for uncoated MPs, large and bright fluorescent spot was found on the stomach of mice at 10 min after intragastric administration (Fig. 4A), showing a rapid release of FITC from uncoated MPs. From 20 to 50 min after intragastric administration, the fluorescence spot enlarged and moved from the stomach to the small intestine and colon part of the nude mice (Fig. 4B-C). This observation indicated a continuous release of FITC from uncoated MPs along the whole GIT. The released FITC could be absorbed into the gastrointestinal tissue and then into the blood circulation system gradually. Thus, from 80 to 180 min after intragastric administration, it can be seen that the fluorescence was spreading with the blood circulation throughout the body (Fig. 4D-F), and the intensity was decreasing due to the metabolism of FITC.

When RS@MPs were used for intragastric administration, the release rate of FITC was found to

be much slower than that of uncoated MPs. At 50 min after intragastric administration, the fluorescent spot remained small, suggesting a quite limited release of FITC from RS@MPs in the upper GIT of mice (Fig. 4C). From 80 to 120 min after intragastric administration, the fluorescent spot was at the colon part of mice and enlarged (Fig. 4D-E). The intensity of fluorescence increased but still not as bright as in the reference group, showing the comparatively slow release rate of FITC from RS@MPs. At 180 min after intragastric administration, the fluorescent spot had spread across the whole body.

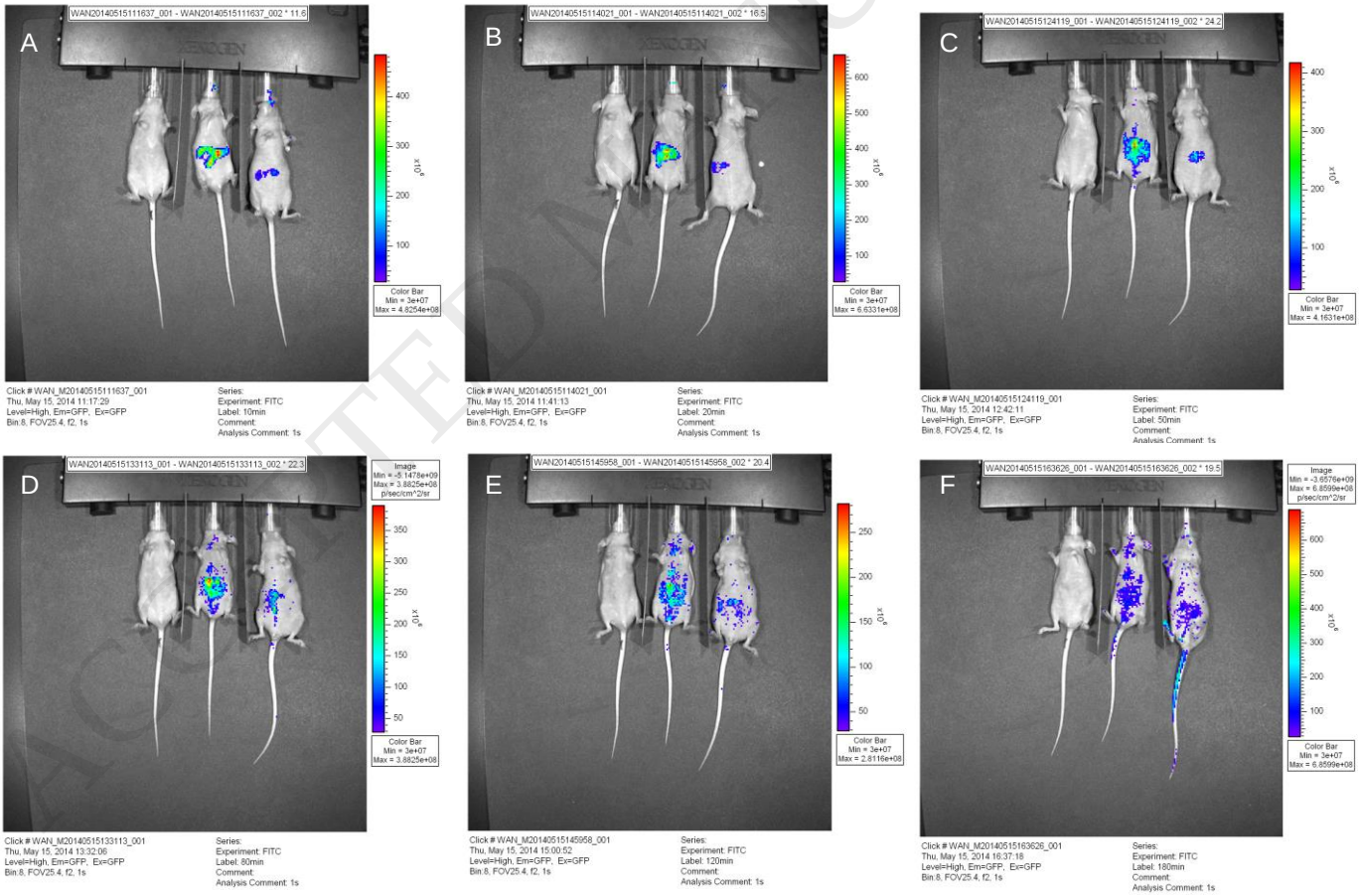

Fig. 4. FITC distribution in the gastrointestinal epithelial tissues for different times (from left to right: blank control, reference and experiment group): (A) 10 min; (B) 20 min; (C) 50 min; (D) 80 min; (E) 120 min; and (F) 180 min.

To further understand the release behavior of RS@MPs, the images showing the FITC distribution in the GIT epithelial tissues of mice after intragastric administration were studied by tissue histospectroscopy. Fig. 5 shows FITC distribution in the GIT epithelial tissues of mice after administration of the uncoated MPs for different times. At 10 min after administration, large and strong fluorescence were found on the stomach and the small intestine epithelial tissues of mice (Fig. 5A-B), indicating the rapid release of FITC from uncoated MPs without the protection of a film. The fluorescence on the stomach and small intestine remained strong up to 40 min after administration (Fig. 5D-E and G-H) because of the continuous release of FITC in the upper GIT and absorption of FITC in epithelial tissues. Along this time, the intensity of fluorescence in the colon epithelial tissues still existed but was weak (Fig. 5C, F, and G), showing no release of FITC in the colon. Here, the weak fluorescence in the colon might be caused by some operation error. At 80 min after administration, the intensity of fluorescence in the colon epithelial tissues enhanced, suggesting the MPs was transported to the colon (Fig. 5L). From 80 min to 24 h, the fluorescence intensity at the colon gradually increased, while the fluorescence intensity of the stomach and small intestine of the mice gradually weakened (Fig. 5M-R). Yet, due to the massive release of FITC in the upper GIT, there was still high fluorescence in the stomach and small intestine tissues.

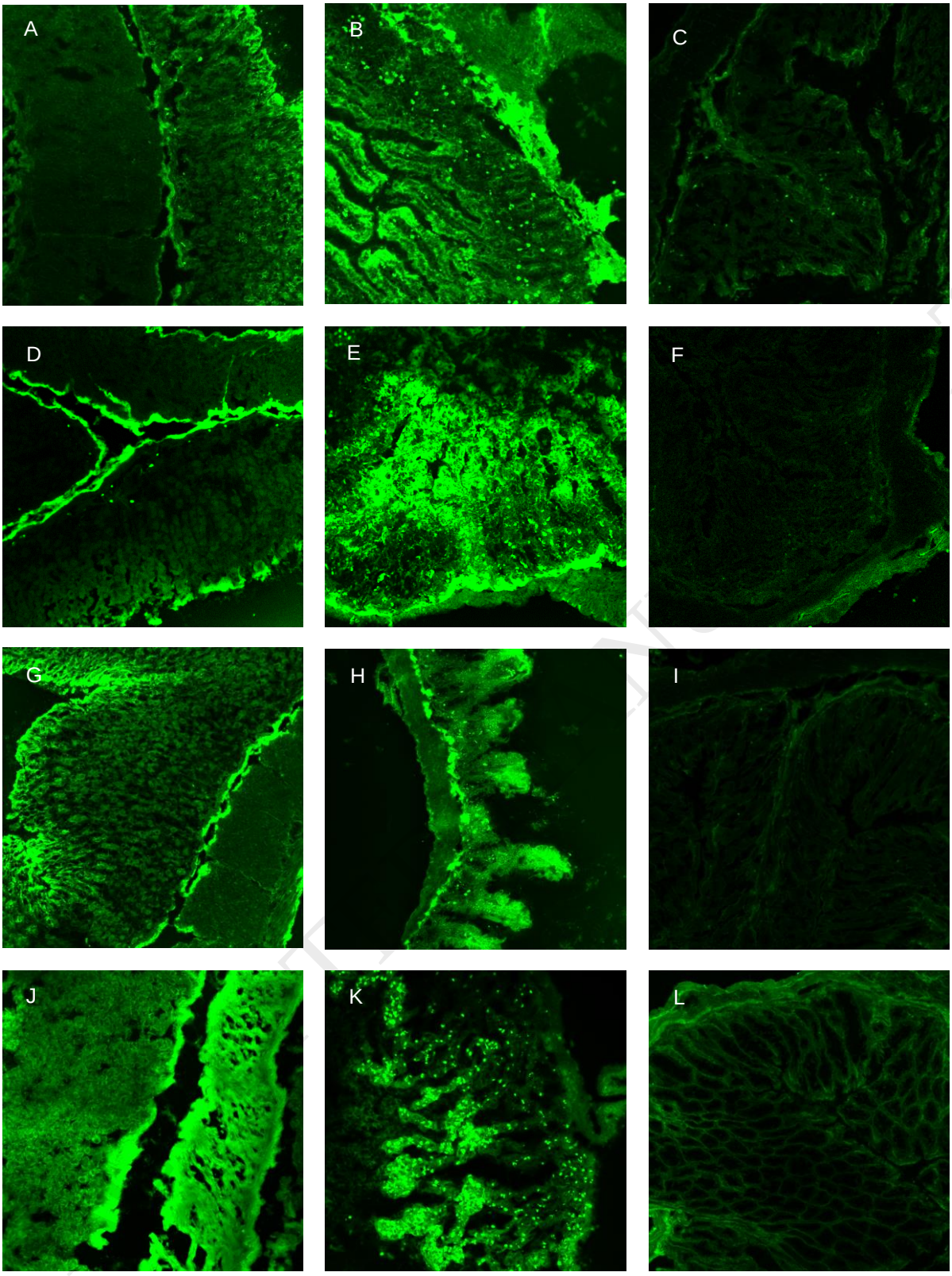

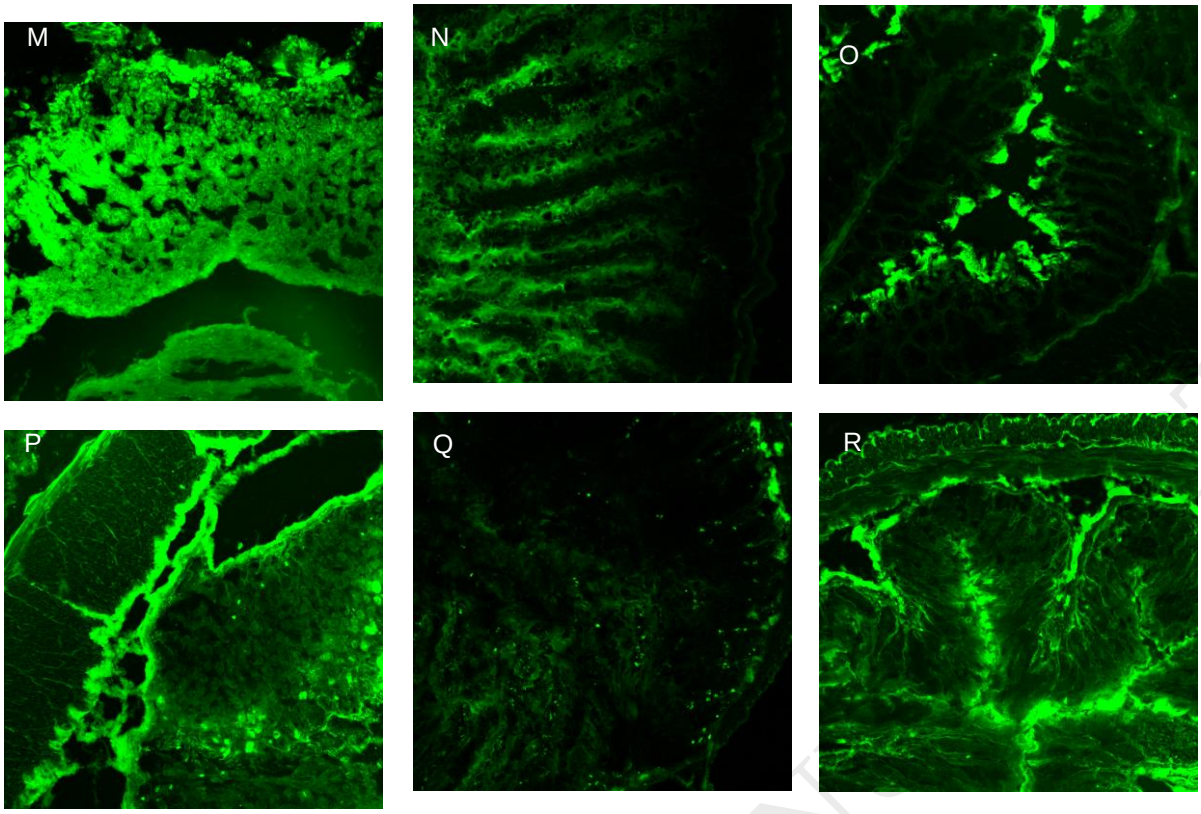

Fig. 5. FITC distribution in the gastrointestinal epithelial tissues of rats after administration of the reference group for different times: (A) stomach, 10 min; (B) small intestine, 10 min; (C) colon, 10 min; (D) stomach, 20 min; (E) small intestine, 20 min; (F) colon, 20 min; (G) stomach, 40 min; (H) small intestine, 40 min; (I) colon, 40 min; (J) stomach, 80 min; (K) small intestine, 80 min; (L) colon, 80 min; (M) stomach, 4 h; (N) small intestine, 4 h; (O) colon, 4 h; (P) stomach, 24 h; (Q) small intestine, 24 h; and (R) colon, 24 h.

Fig. 6 shows the FITC distribution in the GIT epithelial tissues of mice after administration of RS@MPs for different times. Compared with the uncoated MPs (Fig. 5), at 10, 20 and 40 min after administration, the intensity of fluorescence in the stomach and small intestine was much weaker (Fig. 6A-B, D-E, and G-H), especially at 10 min after administration, suggesting the RS2/RS3 film had high resistibility and inhibited the FITC release in the upper GIT. Moreover, there was almost no fluorescence in the colon tissues (Fig. 6A-B, D-E, and G-H). Similar to the uncoated MPs, from 80

min to 24 h after administration, the colon epithelial tissues showed fluorescence and this fluorescence became more intense (Fig. 6L, O, and R). Moreover, compared with the uncoated MPs (Fig. 5L and O), the intensity of fluorescence was comparatively stronger (Fig. 6L and O). This observation clearly indicates the enhanced release of FITC from RS@MPs, which may be due to the fermentation of RSs by anaerobic microflora in the colon (Rubinstein, 1990). These results clearly demonstrate that RS@MP had a colon-targeted property and well-controlled release behavior.

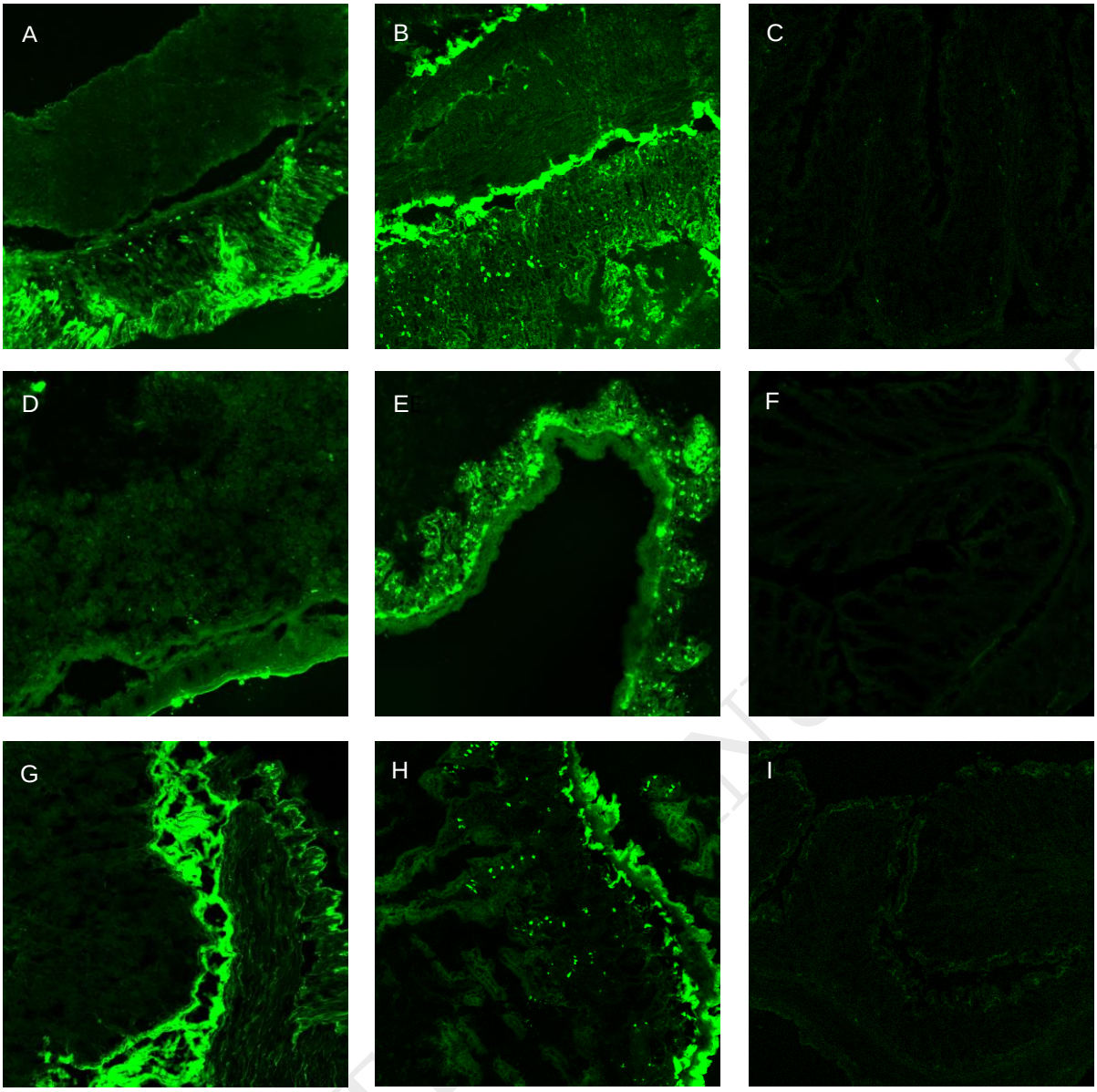

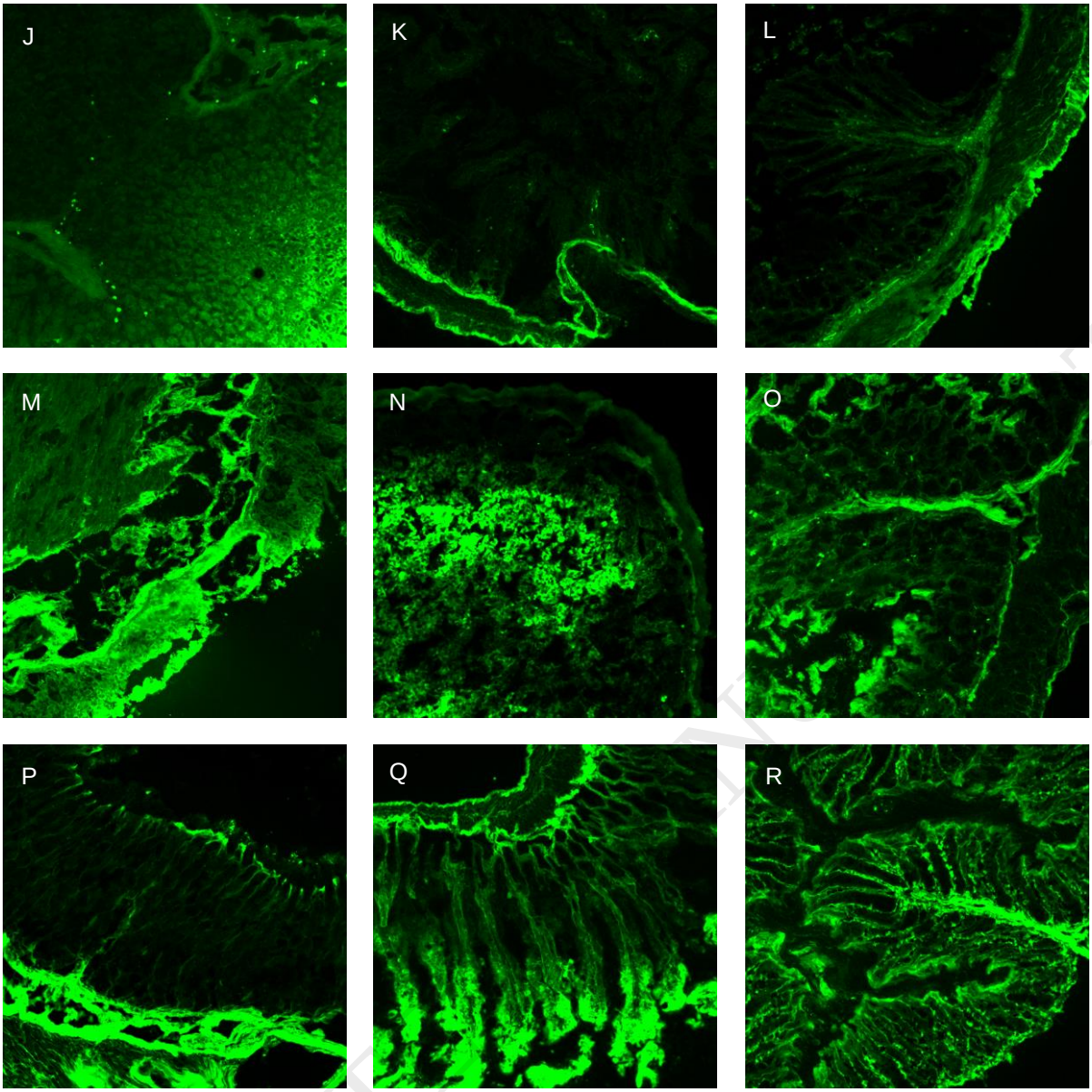

Fig. 6. FITC distribution in the gastrointestinal epithelial tissues of the experiment group for different times: (A) stomach, 10 min; (B) small intestine, 10 min; (C) colon, 10 min; (D) stomach, 20 min; (E) small intestine, 20 min; (F) colon, 20 min; (G) stomach, 40 min; (H) small intestine, 40 min; (I) colon, 40 min; (J) stomach, 80 min; (K) small intestine, 80 min; (L) colon, 80 min; (M) stomach, 4 h; (N) small intestine, 4 h; (O) colon, 4 h; (P) stomach, 24 h; (Q) small intestine, 24 h; and (R) colon, 24 h.

4. Conclusion

The developed method based on RS2/RS3 film is safe and simple, aiming at starch-only-film-coated colon-specific DDSs by physical modification. RS2 came from high-amylose starch particles with a smooth surface and B-type crystalline structure. RS3 with high crystallinity was generated by the recrystallization of starch molecules with suitable M_w. Thus, the resistibility of the coating film was improved by RS2 and recrystallized RS3 to hinder the active compound release. Moreover, for the formation of RS2/RS3 film, RS3 paste acted as a binder. Importantly, for RS@MPs, desired colon-targeted release performance can be easily obtained by adjusting the content of RS2 and RS3 as well as the film-coating thickness of the coated RSA film. This study shows the ability of the newly developed starch-based coating to effectively delivery active compounds (*e.g.*, 5-ASA) into the colon.

Acknowledgments

This research has been financially supported by the National Natural Science Foundation of China (NSFC)–Guangdong Joint Foundation Key Project (U1501214), and YangFan Innovative and Entrepreneurial Research Team Project (2014YT02S029). J. Chen also would like to thank the Guangzhou Elite Project (GEP) for providing research funding for her visiting studies at The University of Queensland (UQ) as part of her PhD work.

References

Bertoft, E., & Manelius, R. (1992). A method for the study of the enzymic hydrolysis of starch granules. *Carbohydrate Research, 227*, 269-283.

Borgquist, P., Zackrisson, G., Nilsson, B., & Axelsson, A. (2002). Simulation and parametric study of a film-coated controlled-release pharmaceutical. *Journal of Controlled Release, 80*(1), 229-245.

Buléon, A., Colonna, P., Planchot, V., & Ball, S. (1998). Starch granules: structure and biosynthesis. *International journal of biological macromolecules, 23*(2), 85-112.

Cheetham, N. W., & Tao, L. (1998). Variation in crystalline type with amylose content in maize starch granules: an X-ray powder diffraction study. *Carbohydrate Polymers, 36*(4), 277-284.

Chen, J., Liang, Y., Li, X., Chen, L., & Xie, F. (2016). Supramolecular structure of jackfruit seed starch and its relationship with digestibility and physicochemical properties. *Carbohydrate Polymers, 150*, 269-277.

Chen, L., Li, X., Li, L., & Guo, S. (2007). Acetylated starch-based biodegradable materials with potential biomedical applications as drug delivery systems. *Current Applied Physics, 7*, e90-e93.

Chen, L., Li, X., Pang, Y., Li, L., Zhang, X., & Yu, L. (2007). Resistant starch as a carrier for oral colon-targeting drug matrix system. *Journal of Materials Science: Materials in Medicine, 18*(11), 2199-2203.

Chen, L., Pu, H., Li, X., & Yu, L. (2011). A novel oral colon-targeting drug delivery system based on resistant starch acetate. *Journal of Controlled Release, 152*, E51-E52.

Chourasia, M., & Jain, S. (2004). Polysaccharides for colon targeted drug delivery. *Drug Delivery, 11*(2), 129-148.

Crowe, T. C., Seligman, S. A., & Copeland, L. (2000). Inhibition of enzymic digestion of amylose by free fatty acids in vitro contributes to resistant starch formation. *The Journal of nutrition, 130*(8), 2006-2008.

Cui, R., & Oates, C. (1999). + The effect of amylose–lipid complex formation on enzyme susceptibility of sago starch. *Food Chemistry, 65*(4), 417-425.

Cummings, J., Milojevic, S., Harding, M., Coward, W., Gibson, G., Botham, R. L., Ring, S., Wraight, E., Stockham, M., & Allwood, M. (1996). In vivo studies of amylose-and ethylcellulose-coated [13 C] glucose microspheres as a model for drug delivery to the colon. *Journal of Controlled Release, 40*(1), 123-131.

Fannon, J. E., Shull, J. M., & BeMiller, J. N. (1993). Interior channels of starch granules. *Cereal chemistry, 70*, 611-611.

Freire, C., Podczeck, F., Veiga, F., & Sousa, J. (2009). Starch-based coatings for colon-specific delivery. Part II: physicochemical properties and in vitro drug release from high amylose maize starch films. *Eur J Pharm Biopharm, 72*(3), 587-594.

Fuentes-Zaragoza, E., Riquelme-Navarrete, M., Sánchez-Zapata, E., & Pérez-Álvarez, J. (2010). Resistant starch as functional ingredient: A review. *Food Research International, 43*(4), 931-942.

Fuentes‐Zaragoza, E., Sánchez‐Zapata, E., Sendra, E., Sayas, E., Navarro, C., Fernández‐López, J., & Pérez‐Alvarez, J. A. (2011). Resistant starch as prebiotic: A review. *Starch‐Stärke, 63*(7), 406-415.

Gérard, C., Colonna, P., Buléon, A., & Planchot, V. (2002). Order in maize mutant starches revealed by mild acid hydrolysis. *Carbohydrate Polymers, 48*(2), 131-141.

Gernat, C., Radosta, S., Anger, H., & Damaschun, G. (1993). Crystalline Parts of Three Different Conformations Detected in Native and Enzymatically Degraded Starches. *Starch - Stärke, 45*(9), 309-314.

Hamman, J. H., Enslin, G. M., & Kotzé, A. F. (2005). Oral delivery of peptide drugs. *BioDrugs, 19*(3), 165-177.

Hari, N., & Nair, A. J. (2016). Development and characterization of chitosan-based antimicrobial films incorporated with streptomycin loaded starch nanoparticles. *New Horizons in Translational Medicine, 3*(1), 22-29.

Haupt, S. M., & Rubinstein, A. (2002). The Colon as a Possible Target for Orally Administered Peptide and Protein Drugs. *19*(6), 53.

Hermans, P., & Weidinger, A. (1948). Quantitative X‐Ray Investigations on the Crystallinity of Cellulose Fibers. A Background Analysis. *Journal of Applied Physics, 19*(5), 491-506.

ISO. (2007). 6647-2:Rice—Determination of amylose content—Part 2.

Iyer, U., Hong, W.-H., Das, N., & Ghebre-Sellassie, I. (1990). Comparative evaluation of three organic solvent and dispersion-based ethylcellulose coating formulations. *Pharm. Technol, 14*(9), 68-86.

Jane, J. L., Wong, K. S., & McPherson, A. E. (1997). Branch-structure difference in starches of A- and B-type x-ray patterns revealed by their Naegeli dextrins. *Carbohydrate Research, 300*(3), 219-227.

Karrout, Y., Neut, C., Wils, D., Siepmann, F., Deremaux, L., Flament, M. P., Dubreuil, L., Desreumaux, P., & Siepmann, J. (2011). Peas starch-based film coatings for site-specific drug delivery to the colon. *Journal of Applied Polymer Science, 119*(2), 1176-1184.

Labastie, M., Solange, A., Brandão, C., & Cumps, J. (1998). *USP-23 dissolution method: A critical evaluation*.

Li, X., Liu, P., Chen, L., & Yu, L. (2011). Effect of resistant starch film properties on the colon-targeting release of drug from coated pellets. *Journal of Controlled Release, 152*, e5-e7.

Lin, Y., Chen, Q., & Luo, H. (2007). Preparation and characterization of N-(2-carboxybenzyl) chitosan as a potential pH-sensitive hydrogel for drug delivery. *Carbohydrate Research, 342*(1), 87-95.

Luengwilai, K., & Beckles, D. M. (2009). Starch granules in tomato fruit show a complex pattern of degradation. *Journal of Agricultural and Food Chemistry, 57*(18), 8480-8487.

Maroni, A., Zema, L., Del Curto, M. D., Foppoli, A., & Gazzaniga, A. (2012). Oral colon delivery of insulin with the aid of functional adjuvants. *Advanced Drug Delivery Reviews, 64*(6), 540-556.

Masuko, T., Minami, A., Iwasaki, N., Majima, T., Nishimura, S.-I., & Lee, Y. C. (2005). Carbohydrate analysis by a phenol–sulfuric acid method in microplate format. *Analytical biochemistry, 339*(1), 69-72.

Milojevic, S., Newton, J. M., Cummings, J. H., Gibson, G. R., Botham, R. L., Ring, S. G., Stockham, M., & Allwood, M. C. (1996). Amylose as a coating for drug delivery to the colon: Preparation and in vitro evaluation using 5-aminosalicylic acid pellets. *Journal of Controlled Release, 38*(1), 75-84.

Oates, C. G. (1997). Towards an understanding of starch granule structure and hydrolysis. *Trends in Food Science & Technology, 8*(11), 375-382.

Ottenhof, M.-A., & Farhat, I. A. (2004). Starch Retrogradation. *Biotechnology and Genetic Engineering Reviews, 21*(1), 215-228.

Palviainen, P., Heinämäki, J., Myllärinen, P., Lahtinen, R., Yliruusi, J., & Forssell, P. (2001). Corn Starches as Film Formers in Aqueous-Based Film Coating. *Pharmaceutical Development and Technology, 6*(3), 353-361.

Planchot, V., Colonna, P., & Buleon, A. (1997). Enzymatic hydrolysis of α-glucan crystallites. *Carbohydrate Research, 298*(4), 319-326.

Pongjanta, J., Utaipattanaceep, A., Naivikul, O., & Piyachomkwan, K. (2009). Debranching enzyme concentration effected on physicochemical properties and α-amylase hydrolysis rate of resistant starch type III from amylose rice starch. *Carbohydrate Polymers, 78*(1), 5-9.

Pu, H., Chen, L., Li, X., Xie, F., Yu, L., & Li, L. (2011). An Oral Colon-Targeting Controlled Release System Based on Resistant Starch Acetate: Synthetization, Characterization, and Preparation of Film-Coating Pellets. *Journal of Agricultural and Food Chemistry, 59*(10), 5738-5745.

Ríos-Covián, D., Ruas-Madiedo, P., Margolles, A., Gueimonde, M., de los Reyes-Gavilán, C. G., & Salazar, N. (2016). Intestinal short chain fatty acids and their link with diet and human health. *Frontiers in microbiology, 7*.

Remon, J. P., Voorspoels, J., Radeloff, M., & Beck, R. H. F. (1996). Starch based drug delivey systems. *Chemical Aspects of Drug Delivery Systems* (pp. 127-137): The Royal Society of Chemistry.

Rubinstein, A. (1990). Microbially controlled drug delivery to the colon. *Biopharmaceutics & drug disposition, 11*(6), 465-475.

Said, A. E.-H. A. (2005). Radiation synthesis of interpolymer polyelectrolyte complex and its application as a carrier for colon-specific drug delivery system. *Biomaterials, 26*(15), 2733-2739.

Sajilata, M. G., Singhal, R. S., & Kulkarni, P. R. (2006). Resistant Starch–A Review. *Comprehensive Reviews in Food Science and Food Safety, 5*(1), 1-17.

Sastry, S. V., Nyshadham, J. R., & Fix, J. A. (2000). Recent technological advances in oral drug delivery – a review. *Pharmaceutical science & technology today, 3*(4), 138-145.

Siccardi, D., Turner, J. R., & Mrsny, R. J. (2005). Regulation of intestinal epithelial function: a link between opportunities

for macromolecular drug delivery and inflammatory bowel disease. *Advanced Drug Delivery Reviews, 57*(2), 219-235.

Sinha, V. R., & Kumria, R. (2001). Polysaccharides in colon-specific drug delivery. *International Journal of Pharmaceutics, 224*(1), 19-38.

Situ, W., Chen, L., Wang, X., & Li, X. (2014). Resistant starch film-coated microparticles for an oral colon-specific polypeptide delivery system and its release behaviors. *Journal of Agricultural and Food Chemistry, 62*(16), 3599-3609.

Thompson, D. B. (2000). Strategies for the manufacture of resistant starch. *Trends in Food Science & Technology, 11*(7), 245-253.

Thompson, L. U., Button, C. L., & Jenkins, D. (1987). Phytic acid and calcium affect the in vitro rate of navy bean starch digestion and blood glucose response in humans. *The American journal of clinical nutrition, 46*(3), 467-473.

Tufvesson, F., Skrabanja, V., Björck, I., Elmståhl, H. L., & Eliasson, A.-C. (2001). Digestibility of starch systems containing amylose–glycerol monopalmitin complexes. *LWT-Food Science and Technology, 34*(3), 131-139.

Vermeylen, R., Goderis, B., Reynaers, H., & Delcour, J. A. (2004). Amylopectin molecular structure reflected in macromolecular organization of granular starch. *Biomacromolecules, 5*(5), 1775-1786.

Vinaykumar, K., Sivakumar, T., Tamizhmani, T., Rajan, T. S., & Chandran, I. S. (2011). Colon targeting drug delivery system: A review on recent approaches. *Int J Pharm, 2*(1), 11-19.

Whistler, R. L., & BeMiller, J. N. (1997). *Carbohydrate chemistry for food scientists*. Eagan press.

Woo, B. H., Jiang, G., Jo, Y. W., & DeLuca, P. P. (2001). Preparation and characterization of a composite PLGA and poly(acryloyl hydroxyethyl starch) microsphere system for protein delivery. *Pharmaceutical Research, 18*(11), 1600-1606.

Zhang, B., Chen, L., Zhao, Y., & Li, X. (2013). Structure and enzymatic resistivity of debranched high temperature–pressure treated high-amylose corn starch. *Journal of Cereal Science, 57*(3), 348-355.

Zhang, G., Ao, Z., & Hamaker, B. R. (2006). Slow Digestion Property of Native Cereal Starches. *Biomacromolecules, 7*(11), 3252-3258.